Finite volume solution of a 2-D heat conduction problem with two sources on a plate

Almério José V. P. S. Pamplona[a]

[a] *Universidade Federal de Goiás, Engenharia Mecânica, Goiânia, Goiás, Brazil*

Abstract

One uses the finite volume method to numerically model 2-D heat conduction with two constant sources on a metallic plate. The paper counts with a code validation, comparing the numerical results with an analytical solution to a simpler problem. After that, one discusses the influence of the heat sources on the plate.

Keywords: Finite Volume Method, Two-dimensions, Heat conduction

1. Introduction

Heat conduction is a significant physical problem in welding, foundry, engines, and many other applications. One can model the phenomena with partial differential equations. However, it is hard, impractical, or impossible to find an analytical solution, depending on the boundary conditions (Morton and Mayers, 2005; LeVeque, 2007; Iserles, 2007). Hence, most engineers and scientists rely on numerical methods to find approximate solutions instead of exact ones. The goal is the insight that they can bring about complex problems. Consequently, that can push scientifical and technological development.

A well-known method is the Finite Volume Method (FVM), based on the integration of the governing equations over infinitesimal volumes (Patankar, 1980; Hirsch, 2007; Versteeg and Malalasekera, 2007). That permits the use of almost any structured or unstructured mesh grid (Moukalled et al., 2016). Furthermore, it has a relatively easy code implementation. As a class exercise, the present paper aims to validate a code using FVM and then apply it to a

Email address: almeriopamplona@gmail.com (Almério José V. P. S. Pamplona)

[1]

specific problem. Thus, one uses a plate with Dirichlet boundary conditions that have an analytical solution for its state. A comparison between the exact and the numerical solution will serve as a validation process. After that, one investigates a plate with two heat sources and external convection.

The work starts with a brief introduction about the governing equations and the problems' discretization using FVM. Then, one presents and discusses the results, concluding the paper with some observations about the examination.

2. Governing Equations

The two-dimensional heat conduction problem is modeled by the parabolic partial differential equation

$$\frac{\partial T}{\partial t} = \alpha \left(\frac{\partial^2 T}{\partial x^2} + \frac{\partial^2 T}{\partial y^2} \right) + S \tag{1}$$

where T is the temperature scalar field, and α is the thermal diffusivity defined as $k/\left(\rho\, c_p\right)$ with k as the thermal conductivity, ρ as the density and c_p as the heat capacity at constant pressure. Additionally, S is an energy source, and x and y are the Cartesian coordinates. A simple application of this problem is a plate with constant temperature on its boundaries, defining a Dirichlet condition. Hence, its proper definition is

$$\begin{aligned}
&\frac{\partial^2 T}{\partial x^2} + \frac{\partial^2 T}{\partial y^2} = 0, \qquad in\,(0,a) \times (0,b) \subset \mathbb{R}^2; \\
&T\,(x,0) = T_s, && \forall x \in (0,a)\,; \\
&T\,(a,y) = T_e, && \forall y \in (0,b)\,; \\
&T\,(x,b) = T_n, && \forall x \in (0,a)\,; \\
&T\,(0,y) = T_w, && \forall y \in (0,b)\,,
\end{aligned} \tag{2}$$

where T_s, T_e, T_n, and T_w are constant temperatures on each side of a rectangular plate with length a and height b. The problem is also represented in Figure 1. One can obtain an analytical solution for Equation (2) using the variable separation method and assuming linearity. The problem's answer can be written as

$$
\begin{aligned}
T(x,y) = \sum_{n=1}^{\infty} \frac{2\,T_s\left[(-1)^{n+1}-1\right]}{n\,\pi}\left[\cosh(\beta\,y) - \coth(\beta\,b)\sinh(\beta\,y)\right]\sin(\beta\,x) + \\
\sum_{n=1}^{\infty} \frac{2\,T_e\left[(-1)^{n+1}-1\right]}{n\,\pi\,\sinh(\lambda\,a)}\sin(\lambda\,y)\sinh(\lambda\,x) + \\
\sum_{n=1}^{\infty} \frac{2\,T_n\left[(-1)^{n+1}-1\right]}{n\,\pi\,\sinh(\beta\,b)}\sin(\beta\,x)\sinh(\beta\,y) + \\
\sum_{n=1}^{\infty} \frac{2\,T_w\left[(-1)^{n+1}-1\right]}{n\,\pi}\left[\cosh(\lambda\,x) - \coth(\lambda\,a)\sinh(\lambda\,x)\right]\sin(\lambda\,y)\,,
\end{aligned}
\tag{3}
$$

where $\beta = (n\,\pi)/a$ and $\lambda = (n\,\pi)/b$.

Figure 1: Rectangular plate with constant temperature on its sides.

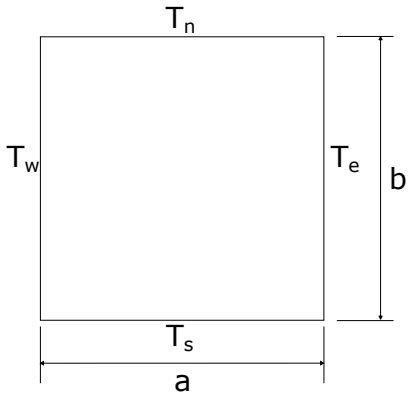

Equation (3) is a result that one uses later to validate the implemented code with FVM. Nonetheless, the present work aims for a more complex application. For instance, consider

$$
\begin{aligned}
&\frac{\partial T}{\partial t} = \alpha \left(\frac{\partial^2 T}{\partial x^2} + \frac{\partial^2 T}{\partial y^2} \right), && in\, [t_0, t_{final}] \times (0,a) \times (0,b) \subset \mathbb{R}^3; \\
&\frac{\partial T}{\partial y}(x,0) = -\frac{Q_{conv}}{k}, && \forall\, x \in [0, 0.15a] \cup [0.40a, 0.60a] \cup [0.85a, a]\,; \\
&\frac{\partial T}{\partial y}(x,0) = -\frac{Q_{source}}{k}, && \forall\, x \in (0.15a, 0.40a) \cup (0.60a, 0.85a)\,; \\
&\frac{\partial T}{\partial x}(a,y) = \frac{Q_{conv}}{k}, && \forall\, y \in [0,b]\,; \\
&\frac{\partial T}{\partial y}(x,b) = \frac{Q_{conv}}{k}, && \forall\, x \in [0,a]\,; \\
&\frac{\partial T}{\partial x}(0,y) = -\frac{Q_{conv}}{k}, && \forall\, y \in [0,b]\,,
\end{aligned}
\tag{4}
$$

where Q_{conv} is the heat due to external convection, and Q_{source} is a constant heat supplied by an external source. The plate is also rectangular with length a and height b. The convection heat can be modeled by Newton's law of cooling,

$$
Q_{conv} = h\, A\, (T_s - T_\infty)\,, \tag{5}
$$

where h is the heat transfer coefficient, T_s is the surface temperature and T_∞ is the neighbour environmental temperature. A simple representation of this problem is in Figure 2.

Figure 2: Rectangular plate with heat source and surfaces exposed to external convection.

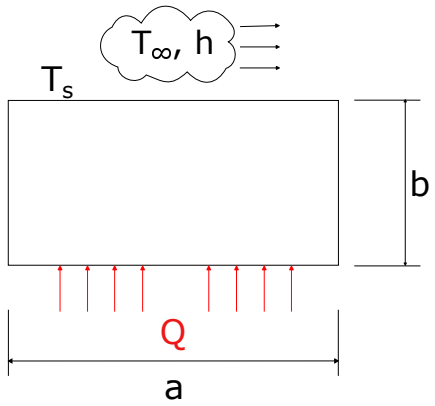

3. Discretization with Finite Volume Method

For both problems in section 2, one discretizes the domain into a uniform collocated mesh. Then, applying the FVM on Equation 1, one obtains

$$T_{i,j}^{n+1} = T_{i,j}^{n} + \frac{\alpha\,\Delta t}{\Delta x^2}\left(T_{i,j+1}^{n} - 2\,T_{i,j}^{n} + T_{i,j-1}^{n}\right) + \frac{\alpha\,\Delta t}{\Delta y^2}\left(T_{i+1,j}^{n} - 2\,T_{i,j}^{n} + T_{i-1,j}^{n}\right), \tag{6}$$

which is the explicit form. The implicit alternative assumes the form of

$$\begin{aligned}\left[1 + 2\,\alpha\,\Delta t\left(\frac{\Delta x^2 + \Delta y^2}{\Delta x^2\,\Delta y^2}\right)\right] T_{i,j}^{n+1} - \frac{\alpha\,\Delta t}{\Delta x^2}\left(T_{i,j+1}^{n+1} + T_{i,j-1}^{n+1}\right) - \\ \frac{\alpha\,\Delta t}{\Delta y^2}\left(T_{i+1,j}^{n+1} + T_{i-1,j}^{n+1}\right) = T_{i,j}^{n},\end{aligned} \tag{7}$$

which is a linear system of equations that requires numerical techniques like Gauss-Seidel or Successive Over-relaxation (SOR) method to solve it. In the present work, one uses the SOR, a faster Gauss-Seidel variant. As an iterative method, the SOR tries to minimize the difference between a previous approximation and the current one. The approximated temperature field is written as

$$\begin{aligned}\hat{T}_{i,j} = \breve{T}_{i,j} - \frac{\gamma}{1 + 2\,\alpha\,\Delta t\left(\frac{\Delta x^2 + \Delta y^2}{\Delta x^2\,\Delta y^2}\right)}\left\{\left[1 + 2\,\alpha\,\Delta t\left(\frac{\Delta x^2 + \Delta y^2}{\Delta x^2\,\Delta y^2}\right)\right]\breve{T}_{i,j} - \right. \\ \left. \frac{\alpha\,\Delta t}{\Delta x^2}\left(\breve{T}_{i,j+1} + \breve{T}_{i,j-1}\right) - \frac{\alpha\,\Delta t}{\Delta y^2}\left(\breve{T}_{i+1,j} + \breve{T}_{i-1,j}\right) - T_{i,j}^{n}\right\},\end{aligned} \tag{8}$$

where $\hat{T}_{i,j}$ and $\breve{T}_{i,j}$ are the current and the previous approximations, respectively. Furthermore, γ is the relaxation constant that regulates the convergence rate. At each iteration, one must guarantee the boundary conditions. From Equation (4), the right, top, and left wall boundaries are written as

$$\begin{aligned}T_{i,N_x} &= \frac{2\,k - h\,\Delta y}{2\,k + h\,\Delta x} T_{i,N_x-1} + \frac{2\,k\,\Delta x}{2\,k + h\,\Delta x}\,T_{\infty}, \\ T_{N_y,j} &= \frac{2\,k - h\,\Delta y}{2\,k + h\,\Delta y} T_{N_y-1,j} + \frac{2\,k\,\Delta y}{2\,k + h\,\Delta y}\,T_{\infty}, \\ T_{i,1} &= \frac{2\,k - h\,\Delta y}{2\,k + h\,\Delta x} T_{i,2} + \frac{2\,k\,\Delta x}{2\,k + h\,\Delta x}\,T_{\infty},\end{aligned} \tag{9}$$

where N_x and N_y are the total cells number, including the ghost cells, on the x-axis and y-axis, respectively. Let's define

$$\Gamma_{conv} = \{x \in \mathbb{R} : x \in [0, 0.15a] \cup [0.40a, 0.60a] \cup [0.85a, a]\}$$

and

$$\Gamma_{source} = \{x \in \mathbb{R} : x \in (0.15a, 0.40a) \cup (0.60a, 0.85a)\}$$

as the bottom boundaries. Now, consider Λ_{conv} the set that contains every $j \in \mathbb{N}$ that maps into a bottom cell whose x-coordinate is in Γ_{conv}. Additionally, consider Λ_{source} the set that has every $j \in \mathbb{N}$ mapped into the boundary with a heat source. The boundaries conditions on the bottom wall are

$$\begin{aligned} T_{1,j} &= \frac{2\,k - h\,\Delta y}{2\,k + h\,\Delta y} T_{2,j} + \frac{2\,k\,\Delta y}{2\,k + h\,\Delta y}\,T_\infty, && j \in \Lambda_{conv} \\ T_{1,j} &= \frac{Q_{source}\,\Delta y}{k} + T_{2,j}, && j \in \Lambda_{source}. \end{aligned} \tag{10}$$

The numerical version of the Dirichlet boundary condition is simpler than the ones represented by Equations 9 and 10. With the artifact of ghost cells, one imposes constant temperature on them, which is enough to guarantee the boundary condition.

4. Results

4.1. Validation

One validated with the problem defined by Equation (1). The boundary conditions were $T_s = 25\,^\circ\text{C}$, $T_e = 50\,^\circ\text{C}$, $T_n = 100\,^\circ\text{C}$ and $T_w = 75\,^\circ\text{C}$. Additionally, the grid had 256×256 cells, the step time was 1.0×10^{-4}, the final time was 60 s, the diffusivity was $3.95 \times 10^{-6}\ m^2/s$, and the plate dimensions were $a = 0.02\ m$ and $b = 0.01\ m$. The temperature distribution of the analytical solution and the numerical simulation are represented in Figures 3a and 3b.

Figure 3: Temperature distribution of the analytical and the numerical solutions.

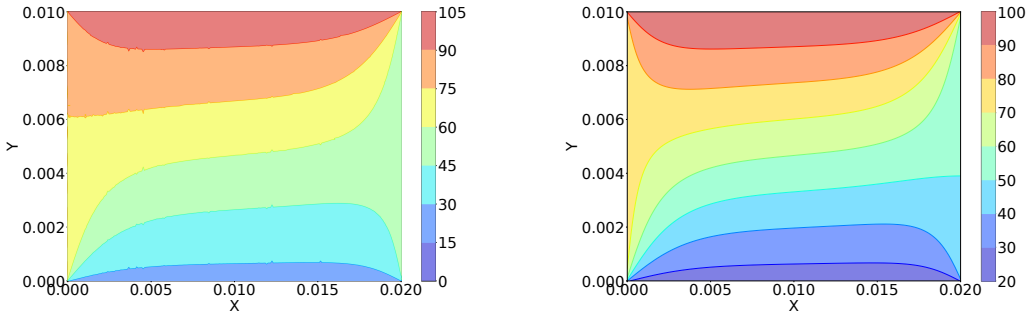

(a) Analytical solution.

(b) Numerical Solution

There are some oscillations in the contours of Figure 3a due to the summation truncation in Equation (3). However, the behavior is consistent, and there is an excellent agreement between the analytical and the numerical solutions. One can further explore the temperature profiles along the middle section of the plate. Figure 4 contains the curves along the x-axis and y-axis.

Observing Figure 4, one notes that the analytical and numerical profiles are very similar. Using the data, one calculates the relative error using

$$E_{L2} = \sqrt{\frac{\sum_{k=1}^{N} \left(\tilde{T}_k - T_k\right)^2}{\sum_{k=1}^{N} T_k^2}} \tag{11}$$

and

$$E_{L1} = \frac{1}{N} \sum_{k=1}^{N} \frac{\mid \tilde{T}_k - T_k \mid}{\mid T_k \mid} \tag{12}$$

where $\tilde{T}$ and T are the numerical and analytical results, respectively, and N is the total number of cells. The calculation results are $E_{L2} = 1.0446\%$ and $E_{L1} = 0.3915\%$, which are expected for a second-order-accurate numerical model. Therefore, the code using the FVM is suitable for heat conduction simulation on plates.

Figure 4: Comparison between the analytical and numerical temperature profiles along the plate's middle section.

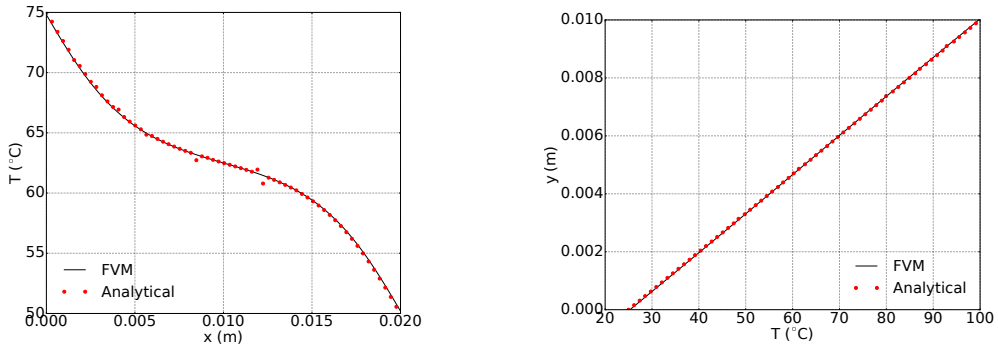

(a) Profile along x-axis.

(b) Profile along y-axis

4.2. Heat Source problem

One chose the following parameters for the heat source problem: a 256×256 grid, $\Delta t = 1.0 \times 10^{-4}$, $t_{final} = 60\ s$, $\alpha = 3.95 \times 10^{-6}\ m^2/s$, $k = 14.9\ W/m\,K$, $h = 20\ W/m^2\,K$, $a = 0.02\ m$, $b = 0.01\ m$ and $Q_{source} = 5 \times 10^4\ W/m^2$. With that criterion, one applied the proposed FVM on Equation (8). Figure 5 shows the temperature distribution on the plate. One depicted the regions with the heat source by the isothermal lines and the color gradient, the red region with 76.3°C.

Furthermore, one notes that the heat diffuses from the heat sources to the environment. Two parabolically isothermal lines represent diffusion. These lines intersect each other in the geometrical center of the plate, forming one quasi-parabolic line. That line becomes flattered as it gets close to the opposite side of the source. This phenomenon shows that, at some point, the external convection over the three boundaries becomes more influential than the heat origin.

Figure 5: Temperature distribution on a plate with two heat sources after 60 s.

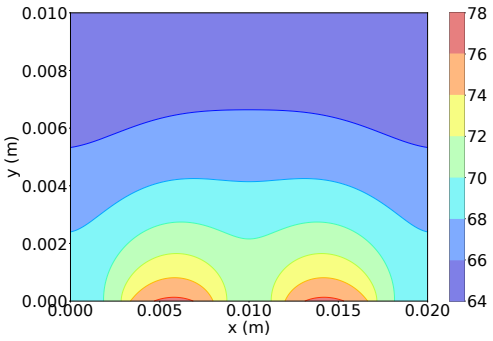

Figure 6a reinforces the intersection between the isothermal lines. The temperature profile is on the plane passing through $(x, 0.005)$, with $x \in [0, 0.02]$. Meanwhile, Figure 6b shows a profile on the plane passing on $(0.01, y)$ with $y \in [0, 0.01]$, a black line, and a contour on the cross-section through $(0.0055, y)$ with $y \in [0, 0.01]$, red circles.

Figure 6: Temperature profile along the plate's middle sections and a cross-section passing through the heat source center.

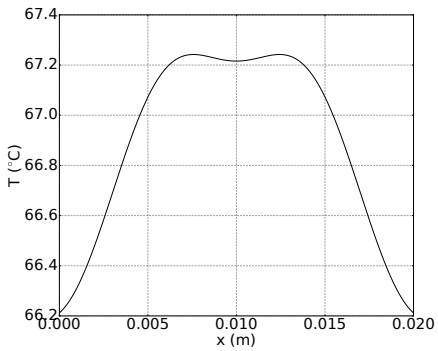

(a) Profile along x-axis.

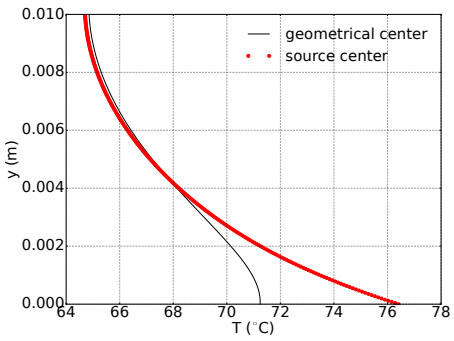

(b) Profile along y-axis

Comparing the two curves, one notes that the heat source influence is significant for $y < 0.004\ m$. However, as one observes the black line, this influence rapidly decreases with the distance because the black line is far from the source and is under the external convection influence too. For $y > 0.004\ m$,

both lines become very similar, probably due to the heat source's low impact and the convection effect.

Additionally, one set of three numerical probes on the plate: one at $(0.01, 0)$, another at $(0.01, 0.005)$, and the last one at $(0.01, 0.01)$. They show that until five seconds, Figure 7, the non-linearity of the time dependent part of the Equation (4) is significant. After that, the temperature increases linearly. Furthermore, the probe on the heat source has the fastest rate at the beginning.

Figure 7: Temperature evolution with time at the probes location.

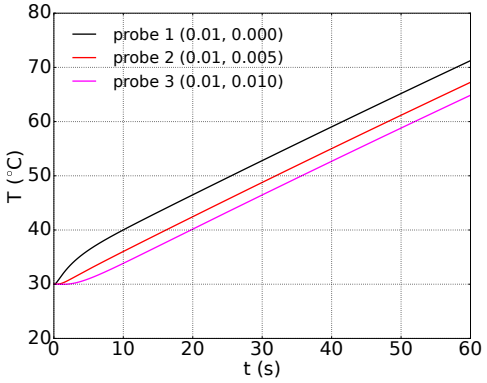

5. Conclusions

The present work did intend to verify the finite volume method applied to heat conduction problems and then apply it to a specific phenomenon. A numerical experiment using a simple two-dimensional Dirichlet boundary problem and comparing it with the analytical solution showed that the model is adequate. After that, one investigated a plate under the influence of two heat sources and external convection. The examination showed that the effects of the heat origin rapidly decreased with the distance leaving space for the convection influence. That is understandable, considering that convection acts on a larger surface area. Furthermore, non-linear effects compose a brief period of the phenomenon, which after $5\,s$ becomes linear.

References

Hirsch, C., 2007. Numerical computation of internal and external flows. 2 ed., Elservier, London.

Iserles, A., 2007. A first course in the numerical analysis of differential equations. 2009 ed., Cambridge University Press, Cambridge.

LeVeque, R.J., 2007. Finite difference methods for ordinary and partial differential equations: Steady-state and time-dependent problems. Society for Industrial and Applied Mathematics, Philadelphia.

Morton, K.W., Mayers, D., 2005. Numerical solution of partial differential equations: An introduction. 2 ed., Cambridge University Press, Cambridge.

Moukalled, F., Mangani, L., Darwish, M., 2016. The finite volume method in computational fluid dynamics: An Advanced Introduction with OpenFoam and Matlab. Springer.

Patankar, S.V., 1980. Numerical heat transfer anad fluid flow. Tatlor and Francis.

Versteeg, H.K., Malalasekera, W., 2007. An introduction to computational fluid dynamics: The finite volume method. 2 ed., Pearso Education Limited, Edinburgh.